AMERICAN SOCIETY FOR MICROBIOLOGY | mBio®

RESEARCH ARTICLE
Host-Microbe Biology

Immune-Mediated Systemic Vasculitis as the Proposed Cause of Sudden-Onset Sensorineural Hearing Loss following Lassa Virus Exposure in Cynomolgus Macaques

Kathleen A. Cashman,[a] Eric R. Wilkinson,[a] Xiankun Zeng,[b] Anthony P. Cardile,[c] Paul R. Facemire,[b]* Todd M. Bell,[b]* Jeremy J. Bearss,[b]* Carl I. Shaia,[b] Connie S. Schmaljohn[d]

[a]Virology Division, U.S. Army Medical Research Institute of Infectious Diseases, Fort Detrick, Frederick, Maryland, USA

[b]Pathology Division, U.S. Army Medical Research Institute of Infectious Diseases, Fort Detrick, Frederick, Maryland, USA

[c]Division of Medicine, U.S. Army Medical Research Institute of Infectious Diseases, Fort Detrick, Frederick, Maryland, USA

[d]Office of the Chief Scientists, U.S. Army Medical Research Institute of Infectious Diseases, Fort Detrick, Frederick, Maryland, USA

ABSTRACT Lassa virus (LASV) causes a severe, often fatal hemorrhagic disease in regions in Africa where the disease is endemic, and approximately 30% of patients develop sudden-onset sensorineural hearing loss after recovering from acute disease. The causal mechanism of hearing loss in LASV-infected patients remains elusive. Here, we report findings after closely examining the chronic disease experienced by surviving macaques assigned to LASV exposure control groups in two different studies. All nonhuman primates (NHPs) developed typical signs and symptoms of Lassa fever, and seven succumbed during the acute phase of disease. Three NHPs survived beyond the acute phase and became chronically ill but survived to the study endpoint, 45 days postexposure. All three of these survivors displayed continuous disease symptoms, and apparent hearing loss was observed using daily subjective measurements, including response to auditory stimulation and tuning fork tests. Objective measurements of profound unilateral or bilateral sensorineural hearing loss were confirmed for two of the survivors by brainstem auditory evoked response (BAER) analysis. Histologic examination of inner ear structures and other tissues revealed the presence of severe vascular lesions consistent with systemic vasculitides. These systemic immune-mediated vascular disorders have been associated with sudden hearing loss. Other vascular-specific damage was also observed to be present in many of the sampled tissues, and we were able to identify persistent virus in the perivascular tissues in the brain tissue of survivors. Serological analyses of two of the three survivors revealed the presence of autoimmune disease markers. Our findings point toward an immune-mediated etiology for Lassa fever-associated sudden-onset hearing loss and lay the foundation for developing potential therapies to prevent and/or cure Lassa fever-associated sudden-onset hearing loss.

IMPORTANCE Lassa virus is one of the most common causes of viral hemorrhagic fever. A frequent, but as yet unexplained, consequence of infection with Lassa virus is acute, sudden-onset sensorineural hearing loss in one or both ears. Deafness is observed in approximately 30% of surviving Lassa fever patients, an attack rate that is approximately 300% higher than mumps virus infection, which was previously thought to be the most common cause of virus-induced deafness. Here, we provide evidence from Lassa virus-infected cynomolgus macaques implicating an immune-mediated vasculitis syndrome underlying the pathology of Lassa fever-associated deafness. These findings could change the way human Lassa fever patients are med-

Received 10 September 2018 **Accepted** 17 September 2018 **Published** 30 October 2018

Citation Cashman KA, Wilkinson ER, Zeng X, Cardile AP, Facemire PR, Bell TM, Bearss JJ, Shaia CI, Schmaljohn CS. 2018. Immune-mediated systemic vasculitis as the proposed cause of sudden-onset sensorineural hearing loss following Lassa virus exposure in cynomolgus macaques. mBio 9:e01896-18. https://doi.org/10.1128/mBio.01896-18.

Editor Diane E. Griffin, Johns Hopkins Bloomberg School of Public Health

Address correspondence to Kathleen A. Cashman, kathleen.a.cashman.ctr@mail.mil, or Connie S. Schmaljohn, connie.s.schmaljohn.civ@mail.mil.

* Present address: Paul R. Facemire, 438th Medical Detachment, Veterinary Service Support, Fort Carson, Colorado, USA; Todd M. Bell, Commander, PHA-Japan, Camp Zama, Kanagawa Prefecture, Japan; Jeremy J. Bearss, Chief, Biological Analysis Division, Landstuhl Regional Medical Center, Landstuhl, Germany.

This article is a direct contribution from a Fellow of the American Academy of Microbiology. Solicited external reviewers: Robert Garry, Jr., Tulane University School of Medicine; Victoria Wahl, National Biodefense Analysis and Countermeasures.

ically managed in order to prevent deafness by including diagnostic monitoring of human survivors for onset of vasculitides via available imaging methods and/or other diagnostic markers of immune-mediated vascular disease.

KEYWORDS Lassa virus, Lassa fever, polyarteritis nodosa, microscopic polyangiitis, vasculitides, autoimmunity, viral infection, viral hemorrhagic fever, cynomolgus macaque, nonhuman primate, deafness, sensorineural hearing loss, brainstem auditory evoked response, virus-associated deafness, anti-neutrophilic cytoplasmic antibodies, ANCA, ANCA-associated vasculitis, autoimmune-associated vasculitis, immune-mediated vasculitis, Lassa virus, autoimmune-associated vasculitis

Lassa fever (LF) is an acute viral hemorrhagic disease endemic to West Africa caused by infection with the rodent-borne arenavirus Lassa virus (LASV). The disease is characterized by fever, malaise, exudative pharyngitis, and retrosternal chest pain that progresses to include mucosal bleeding, severe hemorrhagic conjunctivitis, peripheral and facial edema, and coagulopathy. LF is fatal in approximately 15% to 20% of cases, with the case fatality rate much higher in some outbreaks (1, 2). Neurological sequelae, including memory loss, ataxia, and neuromuscular pain, are common in both mild and severe cases. Most notably, permanent unilateral or bilateral sudden-onset sensorineural hearing loss is observed in an unusually high percentage (approximately 30%) of LF survivors (3–7). The incidence rate of deafness associated with LF greatly exceeds that of any other viral disease known to cause postnatal deafness. For example, the most commonly occurring viral disease known to cause deafness is mumps, in which deafness occurs in less than 0.1% of cases (approximately 300 times less than that of LF) (8). LF-associated deafness is a considerable cause of disability in the regions of West Africa (Nigeria, Liberia, Guinea, and Sierra Leone) where the disease is endemic (9). Since most confirmed cases of LF-associated hearing loss are identified during the convalescent phase in recovering patients and after LASV seroconversion, it has been speculated that hearing loss may be the result of an immune response to infection (10). More recent studies, however, assert that sudden-onset sensorineural hearing loss can also occur during the acute phase of disease, indicating that direct damage due to viral infection may also contribute to hearing loss (11). In a prospective study, five of 37 LF patients experienced hearing loss during the acute phase of infection, and four of those five patients died from LF (11). While the sample size was small in this study, sensorineural hearing loss occurring during the acute phase of disease was more often associated with a fatal outcome (11). Although a clear cause-and-effect relationship between LF and deafness is evident, the underlying pathology has not yet been identified.

Several nonhuman primate (NHP) species have been used to study the pathogenesis of LASV, including cynomolgus macaques, which develop severe and usually fatal disease with signs and pathology mirroring observations from fatal LF cases in humans (12). Typically, macaques develop an acute disease approximately 10 days after infection, which is characterized by fever, malaise, loss of appetite, and reduced activity. Severe disease signs that require euthanasia often occur approximately 11 to 18 days postexposure (dpe). NHPs that survive this acute phase may go on to develop signs characteristic of neurologic damage, including tremors, ataxia, and seizures, which can be fatal in some NHPs. A recent publication describes the subjective determination of sensorineural hearing loss in a STAT1 knockout mouse model following Lassa virus exposure (13). Anecdotal evidence has suggested that NHPs, like humans, can become deaf after surviving LASV infection; however, to date, neither an objective measurement of deafness in primates nor the underlying cause of the deafness in macaques or in humans has been described.

Here we report for the first time the use of an auditory measurement of LASV-associated sensorineural hearing loss in cynomolgus macaques. Moreover, we describe pathological findings indicating that an immune-associated systemic vasculitis disorder is likely to be the basis of LF-associated deafness.

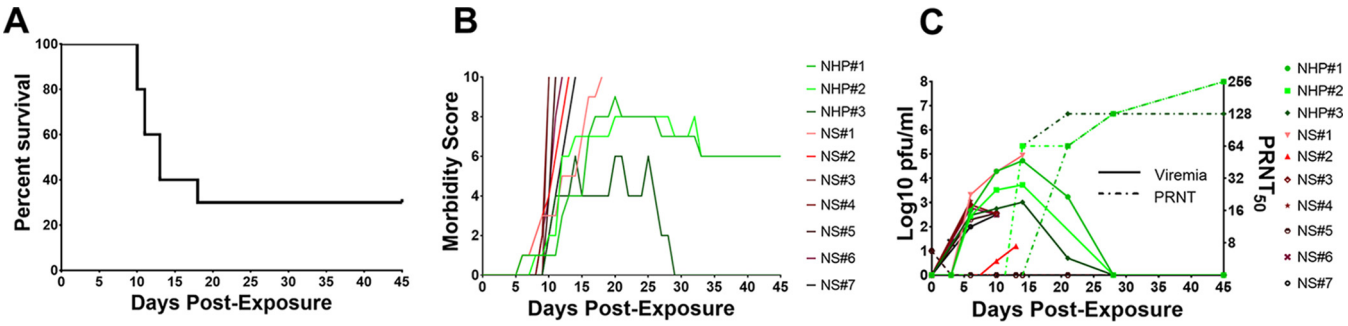

FIG 1 Cynomolgus macaque study outcomes in survivors (denoted in shades of green) versus nonsurvivors (denoted in shades of red). (A) NHPs were infected by IM injection of 1,000 PFU of LASV at day 0 and were observed daily for 45 days. All ten NHPs exhibited signs of disease approximately 6 days postinfection with seven NHPs reaching the euthanasia criteria on days 13 to 18. (B) Morbidity scores were assigned to the NHPs each day with 0 indicating no observable disease signs and 10 indicating severe disease signs requiring euthanasia. The two NHPs that survived to the study endpoint experienced severe disease signs, which did not resolve but did not require euthanasia. Signs of disease included loss of appetite, reduced activity, hunched posture, labored breathing, and neurological deficits, including trembling, muscle weakness, and ataxia. (C) Serum viremia was determined by plaque assay and is expressed in $\log_{10}$ PFU/ml. Development of neutralizing antibodies was measured by plaque reduction neutralization test (PRNT). Titers are expressed as the reciprocal serum dilution required to reduce the number of plaques by 50% ($PRNT_{50}$).

RESULTS AND DISCUSSION

LASV infection of cynomolgus macaques. To determine whether macaques surviving LASV infection develop deafness, we experimentally infected 10 cynomolgus macaques and observed them for 45 days. A daily score was assigned to each macaque corresponding to the severity of disease signs observed. A score of 0 indicated that the macaque was well and showed no signs of disease, and a score of 10 indicated that the macaque was severely ill and required euthanasia. All macaques developed signs of LASV disease by 6 dpe, and seven macaques escalated to meet established euthanasia criteria by 13 and 17 dpe, respectively (Fig. 1A). The morbidity scores of these macaques reflect the time course of disease, which became severe approximately 9 dpe in all ten, increasing steadily in severity for the seven that succumbed, but stabilizing in the three survivors approximately 16 dpe (Fig. 1B). Two of the macaques that survived the acute phase of disease improved slightly by approximately 28 dpe but continued to demonstrate signs of disease, including hunched posture, reduced appetite, tremors, and ataxia that persisted through the end of the study (Fig. 1B). The condition of the third surviving macaque was similar to that of the other two survivors until beginning to improve after day 28, but this NHP was still below his starting weight at the end of the study (45 dpe). Blood samples collected on study days 0, 3, 6, 10, 14, 21, 28, and 45 postexposure were tested for infectious LASV by standard plaque assay and for neutralizing antibody responses by plaque reduction neutralization test (PRNT). All macaques had detectable serum viremia by 6 dpe. Macaques that succumbed had very high viral titers at the terminal blood collection (up to approximately 1×10^7 PFU/ml). Serum viremia levels peaked in the survivors at 14 dpe, followed by clearance of detectable virus in serum by 28 dpe (Fig. 1C). Viral clearance correlated with a rise in neutralizing antibodies in all three survivors (Fig. 1C).

Pathological findings in NHPs are consistent with autoimmune-associated vasculitis in humans. Necropsy of the macaques euthanized during the acute phase of disease, as well as the survivors, revealed gross pathological findings consistent with earlier reports of LASV infection of macaques, which included changes in the lungs, liver, spleen, heart, pancreas, lymph nodes, kidneys, and brain (12, 14). Additionally, the survivors displayed severe gross lesions similar to those reported for human autoimmune-associated vasculitis, specifically in polyarteritis nodosa (PAN) and microscopic polyarteritis (MPA) patients (Fig. 2). The surviving macaques experienced marked thickening of blood vessels in numerous organ systems, including the liver, pancreas, and heart (Fig. 2A, B, and D). The coronary vessels exhibited a segmental vascular dilation and stenosis having a "string of beads" or "rosary sign" appearance as previously described for vasculitis lesions that are often visualized in living subjects radio-

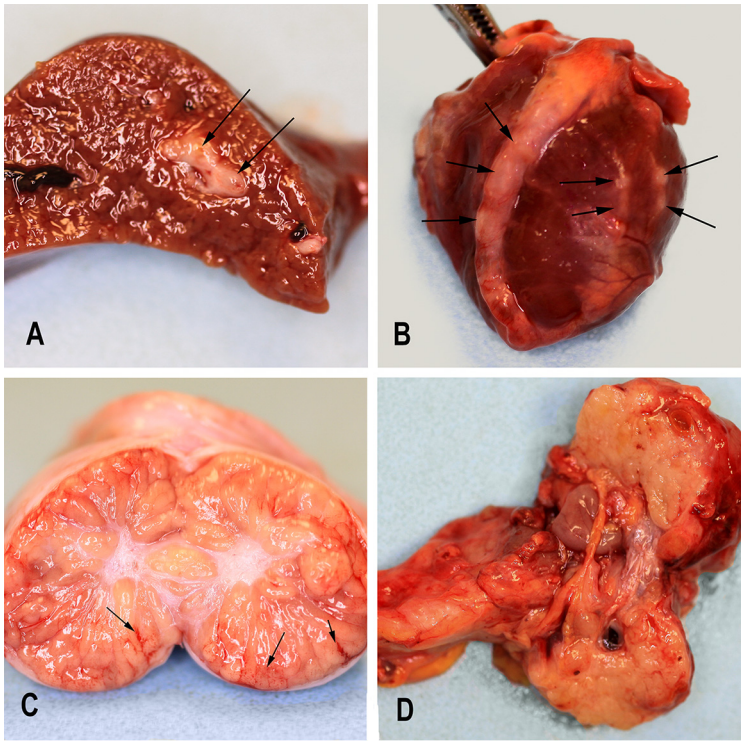

FIG 2 Gross pathology findings from the two macaques surviving LASV exposure. (A) Marked thickening of hepatic vessels in NHP#2 survivor. (B) The coronary vessels exhibiting similar incremental vascular dilation and stenosis having the "string of beads" or "rosary sign" appearance reported for polyarteritis/vasculitis lesions (15). (C) Multiple foci of interstitial testicular hemorrhage in NHP#1 survivor. (D) A white, fibrous, and nodular pancreatic mass in NHP#1, consistent with previous descriptions for PAN patients (18, 19).

graphically and are diagnostic for PAN and other vasculitis syndromes (Fig. 2B) (15). The two male survivors experienced severe testicular edema during the in-life portion of the study, starting approximately 14 dpe, and persisting until the end of the study (45 dpe). At necropsy, gross examination of the testicles revealed evidence of interstitial hemorrhage (Fig. 2C), consistent with autopsy findings in male patients with autoimmune vasculitis (16, 17). Pancreatic lesions are rare in autoimmune vasculitis, but they have been described, specifically, for PAN (18, 19). NHP#1 had a white, fibrous, and nodular pancreatic mass consistent with these descriptions (Fig. 2D). None of the gross lesions observed in the surviving macaques are typically described for acute LASV disease in primates; thus, we propose that they are associated with the development of an immune-associated vasculitis after the acute phase of disease and after viral clearance from the blood.

In addition to the gross findings, we also observed vascular lesions in most organ systems similar to histologic findings reported in human cases of autoimmune-associated vasculitis (Fig. 3A to I). Some autoimmune-associated vasculitides, including PAN, MPA, and cryoglobulinemia in humans, are characterized by necrotizing vasculitis in most organ systems more specifically described as segmental fibrinoid necrosis and profound infiltration of polymorphonuclear neutrophils and monocytes (20, 21). Histopathology performed on tissue samples from the LASV survivors in this study demonstrate similar types of lesions and infiltrates (Fig. 3A and D to H). Proliferative vasculitis was identified in the livers of all survivors (Fig. 3A and B). Examination of the lungs of the survivors revealed interstitial fibrosis with type II pneumocyte hyperplasia but no evidence of proliferative vasculitis. Pneumocyte hyperplasia is a common finding in LASV-exposed guinea pigs and primates that succumb to disease; thus, we believe this is likely due to the primary LASV infection and unrelated to the postexposure immune

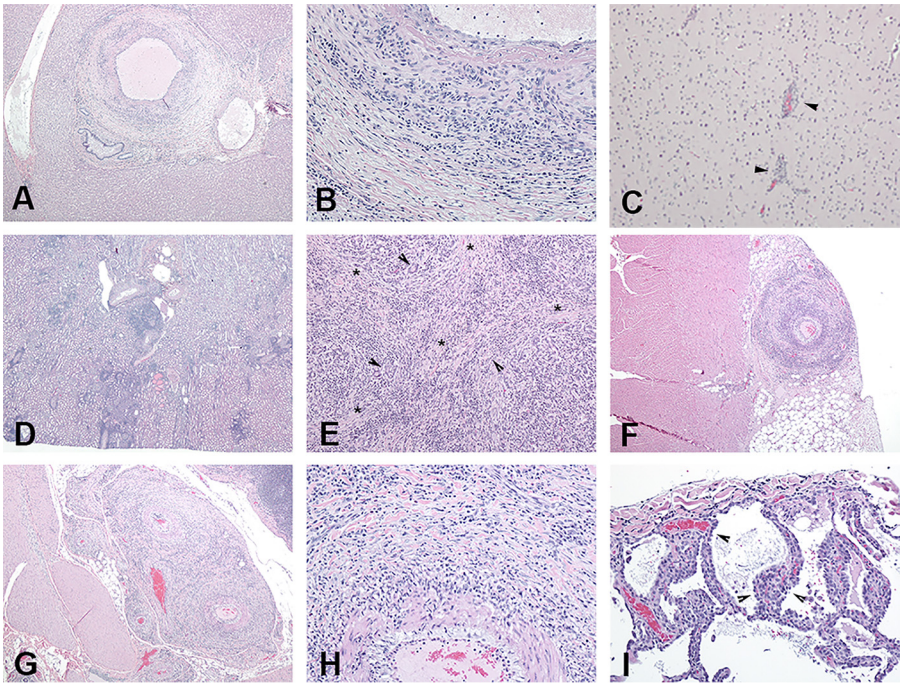

FIG 3 Histopathologic findings in NHPs that survived to the end of study, 45 dpe. (A) Necrotizing and proliferative vasculitis, liver, 45-day surviving NHP, 4×. (B) 20× view of the liver section in panel A. (C) Development of lymphoplasmacytic perivascular encephalitis (denoted by arrowheads) apparent in a nonhuman primate that succumbed after acute phase, 18 dpe, 10×. (D) Membranous glomerulonephritis and vasculitis, kidney, 45-day survivor, 20×. (E) Profound chronic-active pancreatitis with fibrosis (denoted by asterisks) and duct hyperplasia (denoted by arrowheads), 45-day survivor, 10×. (F) Necrotizing and proliferative arteritis with narrowed lumen in the coronary artery, 45-day survivor, 10×. (G) Necrotizing and proliferative arteritis with narrowing of the lumen in the mesenteric artery, 45-day survivor, 4×. (H) Higher magnification of vascular changes noted in panel G, 20×. (I) Interstitial fibrosis with type II pneumocyte hyperplasia (denoted by arrowheads) in the lung tissue of a surviving NHP 45 dpe.

syndrome experienced by this macaque. We were able to observe minor perivascular lesions in the brain of a primate that survived beyond the acute phase of disease but succumbed on day 18 dpe. Similar lesions were not identified in NHPs that succumbed earlier, during the acute phase. An inconsistency with the case definition for PAN in humans is the fact that we identified membranous glomerulonephritis characterized by expansion of the glomeruli with eosinophilic material, lymphoplasmacytic inflammation, degenerate neutrophils, tubular degeneration, necrosis, and regeneration, and eosinophilic proteinaceous casts present in the survivors (Fig. 3D). The proliferative vasculitis identified in the kidneys is similar to that described in the liver and pancreas, with no corresponding immunoreactivity to LASV. It is unknown whether this glomerulonephritis occurred due to the initial exposure to LASV and was resolving or whether it was an active process mediated by the host immune response.

Given the profound inflammatory findings described above in most tissues of the surviving NHPs in the absence of circulating virus or evidence of viral antigen in tissues, we sought a more sensitive method to interrogate the tissue samples for viral persistence. We adapted an *in situ* hybridization method using LASV-specific RNA probes and were able to identify viral genomes present within the arteries with perivascular inflammatory lesions in numerous organs, including the brain, heart, kidney, and liver (Fig. 4). We next sought to identify the cell types persistently infected with LASV via an immunofluorescence assay. Figure 5 shows that smooth muscle cells of arteries, identified by an alpha smooth muscle cell actin-specific antibody marker (Fig. 5B, in red), and not endothelial cells, identified by a CD-31-specific antibody marker (Fig. 5A, in red), remain persistently infected with LASV. However, we cannot determine whether the virus present in the smooth muscle cells is actively replicating or not based on these assays.

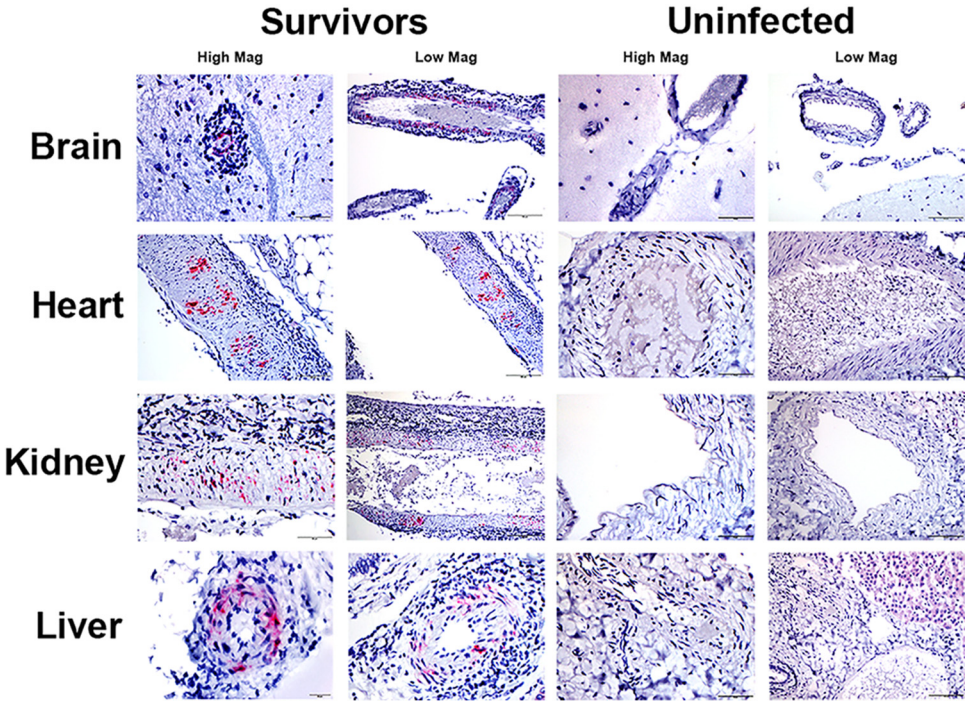

FIG 4 Evidence of persistence of LASV RNA in perivascular lesions of multiple tissues after clearance of circulating virus. A nucleic acid probe corresponding to the sequence 466-1433 of the L segment (within the polymerase gene) of LASV was used to detect nucleic acid with a complementary sequence. Tissue-matched uninfected controls were included to rule out nonspecific binding. Viral genomic RNA was detected in the arteries with perivascular lesions in brain, heart, kidney, and liver 45 dpe. Higher-magnification images are shown in the left columns for survivors and uninfected NHPs, and lower-magnification images are shown in on the right columns.

Auditory response measurements in NHPs that survive LASV infection. By 28 dpe, all three survivors appeared to develop hearing loss based on subjective measurements of sound response and tuning fork tests. Screening for sensorineural hearing loss was conducted on day 45 by measuring brainstem auditory evoked response using an analog audiometer (BAERCOM). The BAERCOM device, developed for use in canines and also used successfully in nondomestic animal species such as elephant seals (personal communication with UFI, Inc. personnel) and alpacas, measures the neural

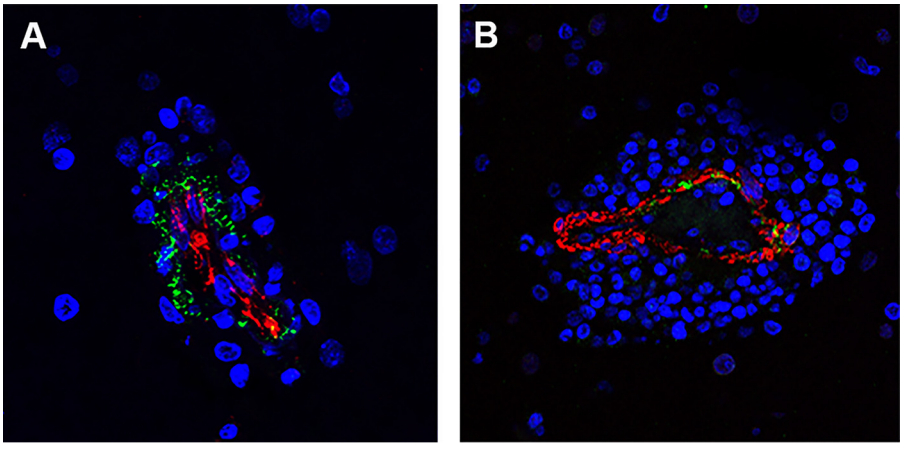

FIG 5 Localization of LASV viral antigen (in green) in the arteries with perivascular lesions in the brain at 45 dpe. (A) The red stain is CD-31, an endothelial cell marker. LASV antigen (in green) can be seen closely associated with, but not within, the endothelium. (B) A smooth muscle cell marker, alpha smooth muscle actin (in red) appears in line with the presence of LASV antigen (in green), indicating that the persistent LASV in the vascular lesions is likely present in the smooth muscle cells.

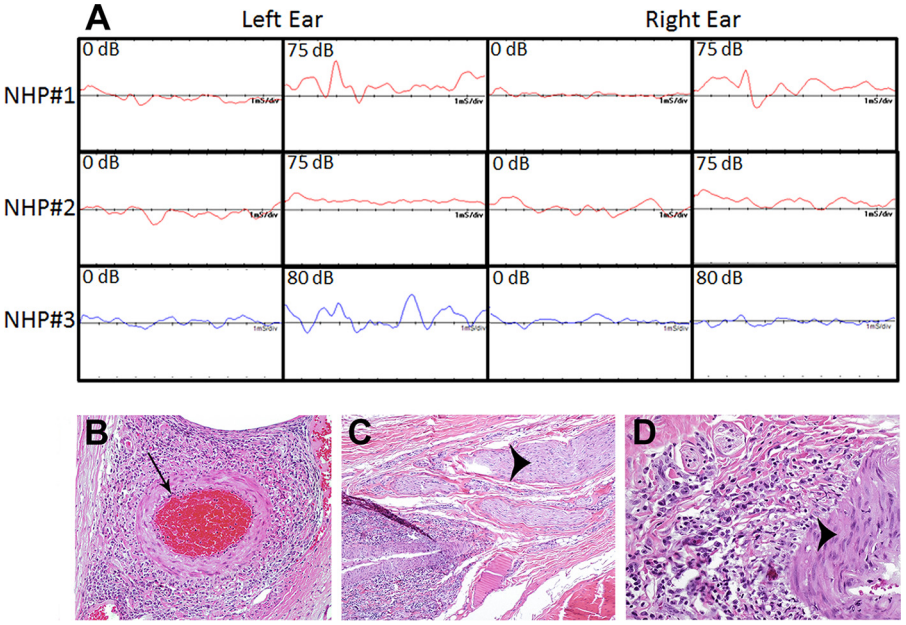

FIG 6 Evidence for sensorineural hearing loss in two surviving NHPs following LASV exposure. (A) A brainstem auditory evoked response device (BAERCOM) was used to assess the surviving NHPs for a hearing response on day 45 postexposure. Clear waveforms indicating a hearing response were observed in both ears of NHP#1 at 75 dB, whereas NHP#2 has an absence of waveforms for both the left and right ears at 75 dB. The third survivor (NHP#3) displays the absence of a waveform in the right ear at 80 dB. (B to D) Histologic examination of the inner ear reveals inflammation of vessels and perivascular tissue at day 45 postexposure. Chronic-active inflammation surrounding a vessel (arrow) at 10× (B) and extending around adjacent nerves (arrowheads) at 10× (C) and at high power (40×) (D).

response to clicking sounds produced at various decibel (dB) levels (22). To our knowledge, this device has not been used with primates prior to this study. Though not an ideal fit for the external auditory anatomy of a primate, we were able to reliably detect normal waveforms in anesthetized healthy, LASV naive primates. The BAERCOM device clearly indicated that two of the three survivors had an absence of waveforms for either both the left and right ears at 75 dB (NHP#2) or the right ear at 80 dB (NHP#3), confirming bilateral and unilateral hearing loss, respectively, in these animals (Fig. 6A). In humans, the auditory threshold is 0 dB, with mild hearing loss diagnosed with a lack of appropriate response at 20 to 40 dB (which is approximately the sound level of quiet conversation). For this study, we were unable to reliably determine an auditory response below 75 to 80 dB in uninfected control animals, likely due to our inability to completely insert the sound-generating ear piece into the ear canal; thus, we established 75 dB or 80 dB (which is approximately the sound level of a busy city street) as the experimental lower limit for measuring deafness in cynomolgus macaques. Though we believe all three of the survivors experienced hearing loss starting approximately 28 dpe and persisting to the end of the study based on subjective measurements of sound response such as a lack of reaction to voice (approximately 60 dB), click sounds (approximately 40 dB), or tuning fork (approximately 40 to 60 dB), one survivor showed a waveform on the BAERCOM device that signified an auditory response at 75 dB for both ears. Refinement of the BAERCOM procedures for NHPs, to reliably measure less profound deafness, would likely increase the number of animals that have confirmed hearing loss. Rapid-onset sensorineural hearing loss is a well-described complication of PAN and other autoimmune-associated vasculitides and is often the presenting symptom. Deafness associated with these vasculitis diseases is believed to be the result of inflammation and occlusion of the anterior inferior cerebellar artery (AICA) and downstream vessels, resulting in cochlear hypoxia (23–29). Consistent with pathological changes seen in humans diagnosed with PAN, tissue samples of the inner ear adjacent to the cochlear nerve of the three surviving NHPs display moderate subacute to

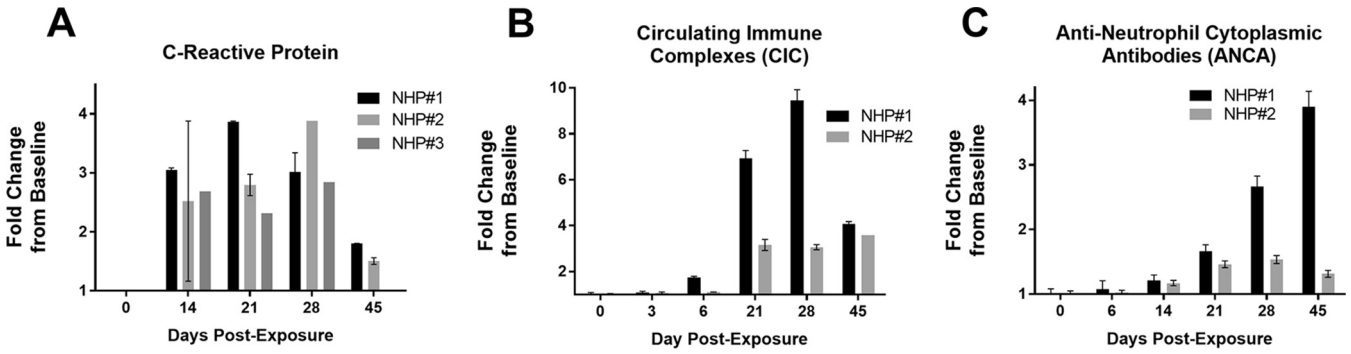

FIG 7 Serological evidence for an autoimmune response in NHPs that survived LASV exposure. (A) C-reactive protein remains high throughout the course of disease for surviving NHPs despite being free of measureable circulating virus in sera by day 28 postexposure. (B) Surviving NHPs experienced a spike in CICs beginning on day 21 postexposure and remained significantly elevated over baseline levels at the end of the study. (C) ANCA was present above baseline levels starting at day 21 postexposure. One NHP experienced a large increase over baseline levels on days 28 and 45 postexposure, whereas the other NHP had levels closer to, but still above, baseline. Sample was not available from NHP#3 for CIC and ANCA analyses.

chronic-active perivascular inflammation which multifocally surrounded smaller branches of the cochlear nerve (Fig. 6B to D) (26). It is important to note that there was no viral staining evident in these sections, but it is impossible for us to determine whether the absence of viral staining is due to the harsh nature of the fixation and decalcification process necessary to remove the bony structures in the inner ear to enable mounting the tissues onto slides for analysis. In addition, there was very little tissue available for mounting on slides once the processing was complete, and no additional tissue was available for testing by the more sensitive methods utilized later, including the *in situ* hybridization and immunofluorescence assays.

Serological profiles of NHPs that survived LASV exposure. There are no definitive tests to diagnose systemic vasculitides; thus, clinical diagnosis is based on the presence of at least three of the following correlative symptoms as delineated by the American College of Rheumatology (ACR): (i) unexplained weight loss; (ii) mottled reticular skin patterns on the extremities or torso; (iii) testicular pain/tenderness; (iv) myalgia, or weakness; (v) mono- or polyneuropathy; (vi) hypertension; (vii) elevated BUN or creatinine; (viii) antibodies to hepatitis B surface antigen in serum; (ix) arteriographic abnormalities; or (x) biopsy specimen of small or medium or large vessels containing polymorphonuclear cells (30). In addition to these criteria, circulating immune complexes (CICs), elevated C-reactive protein, elevated proinflammatory cytokines, or sudden-onset, unexplained sensorineural hearing loss support a clinical diagnosis of systemic vasculitides. Further refinements of the clinical diagnosis criteria for vasculitides were established at the second International Chapel Hill Consensus Conference on the Nomenclature of Systemic Vasculitides in 2012 (31, 32). As a result of this conference, the presence of antineutrophil cytoplasmic antibodies (ANCA) distinguishes PAN from microscopic polyarteritis (MPA).

To obtain confirmatory serological evidence consistent with an aberrant immune response in the survivors, we tested blood samples from two of the three surviving NHPs for immune markers indicative of a systemic autoimmune-associated vasculitis diagnosis in humans. Sample volume limitations prevented us from performing these assays for the third surviving NHP, and the absence of samples beyond the acute phase prevented us from performing all tests on samples from the macaques euthanized due to severe LASV disease. Of the two macaques we tested, we found that both survivors had elevated levels of C-reactive protein in the blood starting at 14 dpe and peaking at 28 dpe despite the absence of measureable virus in the blood at that time (Fig. 7A). After 28 dpe, C-reactive protein levels decreased slightly but remained elevated through the end of the study. CICs are generally very low or undetected in healthy individuals but can become highly elevated in individuals with autoimmune disease, and their presence is often diagnostic. Macaques that succumbed during the acute phase did not develop measureable CICs (data not shown). However, the three survi-

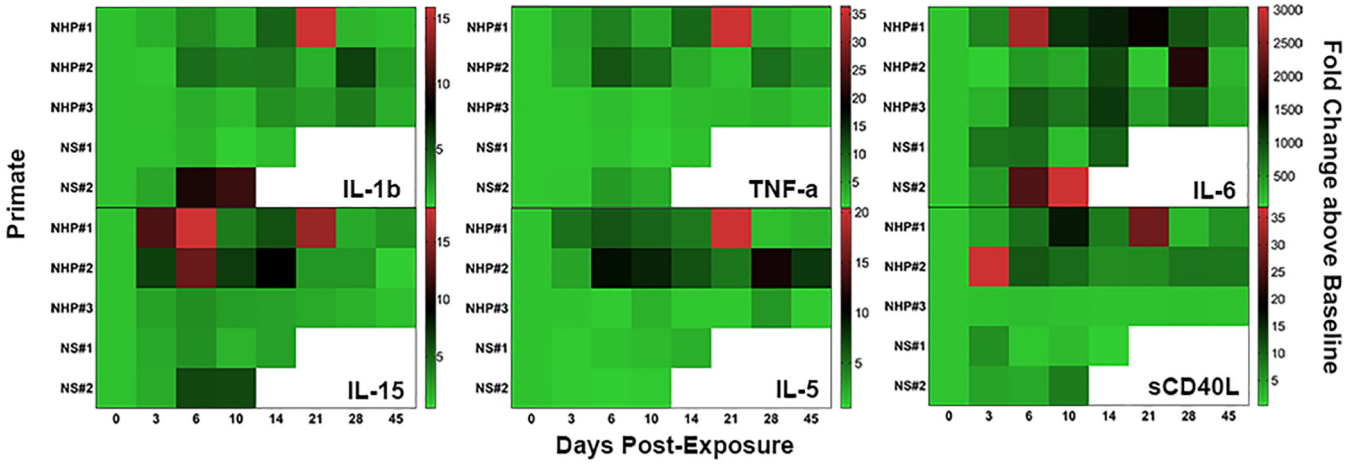

FIG 8 Heat map representation of cytokine and chemokine changes that support a systemic autoimmune response hypothesis. Proinflammatory cytokines IL-1β, TNF-α, and IL-6 became elevated in the acute phase of disease but remained above baseline after viral clearance. Autoimmune mediators IL-15 and IL-5 became strongly elevated during the acute phase of disease in the NHPs that survived, but not in the NHPs that succumbed. IL-15 returned to baseline, and IL-5 differentially returned to baseline by the end of study, with the deaf NHP retaining highly elevated levels. sCD40L became highly elevated early postexposure and remained elevated from baseline throughout the study. All data are presented as fold change from baseline levels. The fold change scale for each cytokine and chemokine is included to the right of each panel.

vors developed highly elevated CICs by 21 dpe, which persisted to the study endpoint. According to the Chapel Hill Consensus Conference, immune complex presence in tissues and in serum suggests a diagnosis of cryoglobulinemic vasculitis (CV), distinguishing CV from both PAN and MPA. However, patients with CV have vasculitis in small vessels only, whereas the macaques in this study had vasculitis lesions in small and medium sized vessels. As such, the presence of high levels of CIC observed in these macaques defies the established human categorization.

Both survivors developed ANCA by 21 dpe, with one demonstrating highly elevated levels on 28 and 45 dpe (Fig. 7C). It is difficult to differentiate between the known vasculitides due to overlapping findings, but based upon the 2012 Chapel Hill Consensus Conference, the presence of ANCA in both survivors, albeit at differing levels above baseline, and the presence of necrotizing glomerulonephritis suggest that the syndrome is similar to MPA, despite the absence of vasculitis in the lungs (Fig. 3D). Cytokines, chemokines, and vascular growth factors that either have been elevated in patients with PAN, MPA, and other similar vasculitides or have been identified as potential therapeutic targets for autoimmune vasculitis were measured and present at elevated levels in the chronically ill macaques. Proinflammatory mediators IL-1β and TNF-α (Fig. 8) became elevated in the surviving NHPs by 3 dpe. IL-1β became highly elevated, approximately 5- to 15-fold increase above baseline, in each of the survivors at different times after 14 dpe, and remained mildly elevated in two survivors at 45 dpe, whereas TNF-α became differentially elevated, with two survivors experiencing increases up to 35-fold above baseline before decreasing to approximately 3- to 8-fold above baseline at 45 dpe. NHP#3 experienced a similar pattern of increase but to a lower magnitude, peaking at approximately a 5-fold increase at day 28. Interleukin 6 (IL-6), a proinflammatory cytokine implicated as a factor in autoimmune disease, became highly elevated from baseline levels in the survivors as early as 3 dpe. NHP#1 experienced a peak of approximately 3,000-fold change above baseline on 6 dpe, and remained consistently high until the end of the study. IL-6 in NHP#2 and NHP#3 experienced a slower increase but became highly elevated, approximately 1,000- to 1,500-fold change above baseline, remaining highly elevated at 28 dpe and returning closer to baseline by the end of study. Cytokines, IL-1β, TNF-α, and IL-6, have all been discussed as potential therapeutic targets for PAN, MPA, and other autoimmune vasculitides, including granulomatosis with polyangiitis (GPA), formerly known as Wegener's granulomatosis and eosinophilic granulomatosis with polyangiitis (EGPA), for-

merly known as Churg-Strauss syndrome (33–38). Other cytokines and chemokines reported to be involved in systemic autoimmune responses include IL-15, IL-5, and sCD40L. Two of the three survivors experienced very high elevations in IL-15, ranging from 10- to 20-fold above baseline, starting as early as 3 dpe, and continuing through 14 and 21 dpe, returning to levels similar to baseline by the end of study (Fig. 8). NHP#3 showed increases that followed the same pattern as the other two survivors but to a lesser magnitude. The normal function of IL-15 is to promote T cell proliferation but also to prevent death of these cells by apoptosis. A potential role for dysregulated expression of IL-15 in autoimmunity is to promote the proliferation and survival of self-reactive lymphocytes (39–42), and IL-15 has been considered a potential therapeutic target for autoimmune diseases such as rheumatoid arthritis and GPA (38, 43, 44). Interestingly, elevated levels (5- to 20-fold increase above baseline) of IL-5, a cytokine that functions to stimulate release of eosinophils into the bloodstream, as well as eosinophilia, were identified in the survivors at 21 and 28 dpe, after viral clearance from the blood (Fig. 8; see also Fig. S1 in the supplemental material). Eosinophils were also noted histologically as a component of the vasculitis in tissues of survivors collected at necropsy (Fig. 3). Another marker of autoimmunity elevated in the survivors was sCD40L, a cytokine and costimulatory molecule with a multitude of important functions in the natural response to infection. Expression of sCD40L is an early marker of T cell activation, and pairing with CD40 cell surface markers on B cells, macrophages, and dendritic cells leads to an enhancement of antigen-specific immune responses. One of the ways in which this task is accomplished is through CD40 and sCD40L complex-mediated bridging of activated T cells and B cells to promote antigen-specific B cell differentiation, isotype switching from IgM to IgG, and memory B cell formation (45, 46). A proposed role for dysregulated and prolonged expression of sCD40L in autoimmunity is activation of self-reactive lymphocytes and prevention of their deletion, which leads to proliferation of autoantibodies (47). We were able to measure highly elevated levels (approximately 35-fold increase above baseline) of sCD40L in serum of NHP#2 as early as 3 dpe. NHP#1 experienced a mild increase on day 3 and continued to exhibit increased sCD40L, peaking at approximately 30- to 35-fold above baseline at 21 dpe. Levels of sCD40L remained above baseline for these survivors throughout the end of the study. In comparison, NHP#3 experienced only mild increases, approximately 5-fold above baseline throughout the study period.

The mixed manifestations of vasculitis observed herein could be described as an "overlap syndrome" which are commonly observed in rheumatologic disease (48). Based on definitions in the Chapel Hill Consensus Conference guidelines, this vasculitis would be considered a "vasculitis that is associated with a probable specific etiology" and thus, Lassa-associated vasculitis (31, 32). It should be noted that it is unknown if human LASV survivors also have such overlapping PAN and MPA markers and similar pathological processes. There is a paucity of human pathology data in Lassa patients, and there have not been any recent studies in humans to our knowledge (49–53). Most of the limited available data do not point to vasculitis in humans who did not survive (49–53). However, in one case series, a patient was described as having congestion and clusters of chronic inflammatory cells around smaller blood vessels and infiltration of some of the vessel walls by chronic inflammatory cells (49). In another case series, four patients were described as having edematous and narrowed liver arterioles and central arteries of the spleen surrounded by fibrinoid material, with vessel wall edema, eosinophilic thickening, and endothelial swelling (50). It is also worth noting that all of the human cases for which pathology samples have been collected and analyzed have been from fatal cases, in contrast to the NHP survivors we have described. It is possible that a Lassa-associated vasculitis syndrome similar to what we have observed in NHPs could occur in human survivors and that it may not have been noted as most Lassa infections occur in resource-limited settings. To determine whether this phenomenon occurs in humans, blood samples could be collected from human survivors of LF to look for biomarkers of vasculities and compared between patients who have hearing loss, or other chronic sequelae, and those that do not. However, establishing a pathological

diagnosis of vasculitis, which would be possible with imaging studies such as those commonly used to identify the rosary bead appearance of vasculitis lesions of patients with PAN and other vasculitis disorders, would be more difficult in human survivors, especially in resource-limited settings, and could be considered if biomarkers lead to suspicion of a vasculitic process.

Conclusions. The surviving macaques in our study displayed seven of the 10 ACR criteria for diagnosis of autoimmune-associated systemic vasculitis in humans. Additionally, they had elevation of all four of the serological markers which are hallmarks of PAN and many characteristics common to MPA and other autoimmune-associated vasculitides, such as the presence of immune complexes in serum, measureable deafness, and histologic lesions commonly observed in systemic vasculitis patients. Our results do not specifically describe or indicate a discrete subcategory of systemic vasculitis; however, these results strongly suggest that an ANCA-positive immune-mediated vasculitis-like syndrome could serve as the underlying cause of rapid-onset sensorineural hearing loss in cases of Lassa fever. Although the number of animals in this analysis is small, the compiled results reflect consistent findings in surviving animals from two distinct studies, indicating that the Lassa fever-associated vasculitis overlap syndrome, as described, is a reproducible finding in our disease model. Continued animal model development will help to further define the cause-and-effect relationship of LASV infection, chronic vasculitis disease, and sensorineural hearing loss. Expanding our understanding of the role of a chronic, aberrant inflammatory immune response in post-acute Lassa fever in primates and how these secondary effects might be prevented could result in enhanced medical management of human cases.

MATERIALS AND METHODS

Primate exposure. Ten adult cynomolgus macaques were infected with an intramuscular target dose of 1,000 PFU of LASV, Josiah strain (14) in sterile physiological saline via a single injection of 1 ml of the virus-containing solution into the quadriceps muscle group. Macaques were monitored daily for disease progression and were euthanized when moribund, according to IACUC-approved euthanasia criteria or at the end of the study period (45 dpe).

Blood sample collection and analyses for viremia, chemistry, and hematology. Blood samples were collected before infection and on days 0, 3, 6, 10, 14, 28, and 45 postexposure from anesthetized macaques. Experiments using samples collected from LASV-infected animals were performed in biosafety level 4 conditions. Viremia was measured by standard plaque assay as previously described (54, 55). Briefly, Vero cells, seeded in 6-well cell culture plates were incubated with 10-fold serial dilutions of each serum for 1 h at 37°C and 5% CO_2, after which an overlay of 0.8% molecular grade agarose in EBME (basal medium Eagle with Earle's salts) fortified with 10% fetal bovine serum and 20 μg/ml gentamicin was applied to each well and allowed to solidify. Cells were then incubated at 37°C and 5% CO_2 for 4 days, and a solution of neutral red (custom blended for USAMRIID by Invitrogen, Carlsbad, CA) was added. After an overnight incubation at 37°C in the stain, plaques were counted and recorded. Chemistry and hematology assessments included measurements of blood glucose, urea nitrogen, creatinine, uric acid, calcium, albumin, total protein, alanine aminotransferase (ALT), aspartate aminotransferase (AST), alkaline phosphatase (AP), total bilirubin, gamma glutamyl transferase, and amylase. Approximately 100 μl of each serum sample was applied to a General Chemistry 13-panel rotor and evaluated in a Piccolo point-of-care blood chemistry analyzer (Abaxis). For the CBC analysis, EDTA-treated whole-blood samples (75 μl) treated with EDTA were aliquoted and run on a Hemavet instrument (Drew Scientific). Results for CBC and chemistry analyses are shown in the figures in the supplemental material.

Evaluation of sensorineural hearing loss. Hearing screenings were performed using a brainstem auditory evoked response communication (BAERCOM) device (UFI, Inc.) according to the manufacturer's instructions. Briefly, needle probes were placed subdermally into the skin above each ear in the area of the temporal bones. An additional probe was placed subdermally on the crown of the head. The probes were plugged into the BAERCOM device, which was set to medium-resolution recording. An earplug was placed into one ear at a time, and audiometric readings were collected at 0 dB to obtain a baseline measurement and at 75 dB for each ear. The BAERCOM software produced graphs for each reading.

Measurement of immune markers. A Raji Cell Immune Complex ELISA (MicroVue CIC-Raji Cell Replacement EIA, Quidel Corp.) was used to measure C3d-bound CIC present in plasma or serum. ANCA antibodies were assessed using an ANCA Screen IgG Test kit (Diagnostic Automation Inc.) that measures levels of anti-myeloperoxidase (anti-MPO) and/or anti-proteinase-3 (anti-PR3) IgG antibody in serum. To measure the circulating levels of C-reactive protein in serum, the Monkey C-Reactive Protein ELISA (Life Diagnostics, Inc.) was utilized. All assays were performed according to the manufacturer's instructions, and results were obtained on a Molecular Diagnostics SpectraMax M5 multimode microplate reader. Cytokine and chemokine assays were performed on plasma samples using a Milliplex MAP Non-Human Primate Cytokine Premixed 23-Plex Immunology Multiplex Assay Magnetic Bead Panel (Merck-Millipore).

The assay was performed according to the manufacturer's instructions, and results were obtained on a Luminex FlexMap 3D instrument.

Pathologic analysis of tissues. Necropsies were performed on each macaque immediately following euthanasia in the USAMRIID biosafety level 4 laboratory. Tissues from major organ systems were collected, immersed and fixed in 10% neutral buffered formalin, and held in biocontainment for a minimum of 21 days. Histopathology samples were routinely processed, embedded in paraffin, sectioned, and stained with hematoxylin and eosin. Immunohistochemistry was performed on replicate tissue sections for both partial and full necropsies using an Envision kit (Dako). A monoclonal antibody specific for Lassa virus GP1 (54) was used at a dilution of 1:15,000. After deparaffinization and peroxidase blocking, an antigen retrieval step was performed using a TRIS/EDTA buffer in a steamer for 30 min. Tissue slides were covered with primary antibody, incubated at room temperature for 30 min, and rinsed. The secondary antibody, a peroxidase-labeled polymer, was applied for 30 min, and the slides were rinsed again. Substrate-chromogen solution (DAB; Dako) was applied for 5 min; the slides were rinsed in distilled water, counterstained with hematoxylin for 2 min, dehydrated, and cleared with xyless, and then coverslips were placed on the slides. Slides were examined with a Nikon Eclipse 600 light microscope.

***In situ* hybridization.** *In situ* hybridization was performed using RNAscope 2.5 HD RED kit according to the manufacturer's instructions (Advanced Cell Diagnostics, Hayward, CA). Briefly, 20 ZZ probes set to target positions 466 to 1433 of the Lassa virus genome with GenBank accession number KM821901.1 were synthesized. After deparaffinization and peroxidase blocking, the sections were heated in antigen retrieval buffer and then were digested by proteinase. The sections were covered with ISH probes and incubated at 40°C in a hybridization oven for 2 h. After the sections were rinsed, ISH signal was amplified using kit-provided Pre-amplifier and Amplifier conjugated to alkaline phosphatase, and incubated with a Fast Red substrate solution for 10 min at room temperature. Sections were then stained with hematoxylin, air dried, and mounted.

Immunofluorescence staining. Formalin-fixed paraffin-embedded NHP tissue sections were deparaffinized and rehydrated through a series of graded ethanol solutions. After 0.1% Sudan black B (Sigma) treatment to quench autofluorescence, the sections were boiled in citrate buffer (pH 6.0) for 15 min to unmask antigen. After rinses with PBS (pH 7.4), the section were blocked with PBS containing 5% normal goat serum overnight at 4°C. Then the sections were incubated with mouse anti-LASSA (USAMRIID, 52-2074-7A) and rabbit polyclonal antibody against CD31 (ab28364; Abcam, Cambridge, MA, USA) at a dilution of 1:100 or rabbit polyclonal antibody against alpha-smooth muscle actin (alpha-SMA, ab5694; Abcam, Cambridge, MA, USA) at a dilution of 1:500 for 2 h at room temperature. After rinses with PBS, the sections were incubated with secondary Alexa Fluor 488-conjugated goat anti-rabbit antibody and Alexa Fluor 561-conjugated goat anti-mouse antibody for 1 h at room temperature. Vectashield mounting medium with DAPI (Vector Laboratories) was placed over the sections, and cover slips were put over the slides. Images were captured on a Zeiss LSM 880 confocal system and processed using ImageJ software.

SUPPLEMENTAL MATERIAL

Supplemental material for this article may be found at https://doi.org/10.1128/mBio.01896-18.

FIG S1, DOCX file, 1.6 MB.

FIG S2, DOCX file, 1 MB.

TABLE S1, DOCX file, 0.02 MB.

ACKNOWLEDGMENTS

Research was conducted under an IACUC-approved protocol in compliance with the Animal Welfare Act, PHS policy, and other federal statutes and regulations relating to animals and experiments involving animals. The facility where this research was conducted is accredited by the Association for Assessment and Accreditation of Laboratory Animal Care International and adheres to principles stated in the 2011 National Research Council's *Guide for the Care and Use of Laboratory Animals*. The BSL-4 facility where this research was conducted is fully accredited by the Association for Assessment and Accreditation of Laboratory Animal Care International.

We thank Heather Esham and Joshua Shamblin for assistance with blood sample collection. Additionally, we are grateful to the technical staff of the Pathology Division for assistance with processing, cutting, and staining tissues for microscopic analysis. We thank Robin Burke for helpful discussions about BAERCOM analysis.

This study was funded by the Military Infectious Disease Research Program (MIDRP).

The opinions, interpretations, conclusions, and recommendations are those of the authors and are not necessarily endorsed by the U.S. Army.

K.A.C. designed the study. K.A.C. and E.R.W. performed all research activities. C.I.S. and J.J.B. performed necropsies. P.R.F., T.M.B., J.J.B., and C.I.S. performed pathological analyses. X.Z. performed *in situ* hybridization and immunofluorescence assays and

contributed to writing those portions of the paper. A.P.C. provided insights into medical practice from a physician's perspective and provided editorial comments. K.A.C. analyzed data. E.R.W., P.R.F., and C.I.S. provided editorial comments. K.A.C. and C.S.S. wrote the paper.

REFERENCES

1. Liang Y, Lan S, Ly H. 2009. Molecular determinants of Pichinde virus infection of guinea pigs–a small animal model system for arenaviral hemorrhagic fevers. Ann N Y Acad Sci 1171:E65–E74. https://doi.org/10.1111/j.1749-6632.2009.05051.x.
2. Branco LM, Grove JN, Boisen ML, Shaffer JG, Goba A, Fullah M, Momoh M, Grant DS, Garry RF. 2011. Emerging trends in Lassa fever: redefining the role of immunoglobulin M and inflammation in diagnosing acute infection. Virol J 8:478. https://doi.org/10.1186/1743-422X-8-478.
3. Cummins D. 1992. Rats, fever and sudden deafness in Sierra Leone. Trop Doct 22:83–84.
4. Liao BS, Byl FM, Adour KK. 1992. Audiometric comparison of Lassa fever hearing loss and idiopathic sudden hearing loss: evidence for viral cause. Otolaryngol Head Neck Surg 106:226–229. https://doi.org/10.1177/019459989210600303.
5. Mateer EJ, Huang C, Shehu NY, Paessler S. 2018. Lassa fever-induced sensorineural hearing loss: a neglected public health and social burden. PLoS Negl Trop Dis 12:e0006187. https://doi.org/10.1371/journal.pntd.0006187.
6. Okokhere PO, Ibekwe TS, Akpede GO. 2009. Sensorineural hearing loss in Lassa fever: two case reports. J Med Case Rep 3:36. https://doi.org/10.1186/1752-1947-3-36.
7. Simmons FB. 1993. Lassa fever and sudden hearing loss. Otolaryngol Head Neck Surg 109:559.
8. Booth J. 1979. Diagnosis and management of sudden fluctuant sensorineural hearing loss, p 737–783. *In* Ballantyne JG, Groves J (ed), Scott-Brown's diseases of the ear, nose, and throat, vol 4. Butterworth's, London, United Kingdom.
9. Rybak LP. 1990. Deafness associated with Lassa fever. JAMA 264:2119. https://doi.org/10.1001/jama.1990.03450160089037.
10. Cummins D, McCormick JB, Bennett D, Samba JA, Farrar B, Machin SJ, Fisher-Hoch SP. 1990. Acute sensorineural deafness in Lassa fever. JAMA 264:2093–2096. https://doi.org/10.1001/jama.1990.03450160063030.
11. Ibekwe TS, Okokhere PO, Asogun D, Blackie FF, Nwegbu MM, Wahab KW, Omilabu SA, Akpede GO. 2011. Early-onset sensorineural hearing loss in Lassa fever. Eur Arch Otorhinolaryngol 268:197–201. https://doi.org/10.1007/s00405-010-1370-4.
12. Hensley LE, Smith MA, Geisbert JB, Fritz EA, Daddario-DiCaprio KM, Larsen T, Geisbert TW. 2011. Pathogenesis of Lassa fever in cynomolgus macaques. Virol J 8:205. https://doi.org/10.1186/1743-422X-8-205.
13. Yun NE, Ronca S, Tamura A, Koma T, Seregin AV, Dineley KT, Miller M, Cook R, Shimizu N, Walker AG, Smith JN, Fair JN, Wauquier N, Bockarie B, Khan SH, Makishima T, Paessler S. 2016. Animal model of sensorineural hearing loss associated with Lassa virus infection. J Virol 90:2920–2927. https://doi.org/10.1128/JVI.02948-15.
14. Jahrling PB, Hesse RA, Eddy GA, Johnson KM, Callis RT, Stephen EL. 1980. Lassa virus infection of rhesus monkeys: pathogenesis and treatment with ribavirin. J Infect Dis 141:580–589. https://doi.org/10.1093/infdis/141.5.580.
15. Lassiter FD. 1998. The string-of-beads sign. Radiology 206:437–438. https://doi.org/10.1148/radiology.206.2.9457197.
16. Stroup SP, Herrera SR, Crain DS. 2007. Bilateral testicular infarction and orchiectomy as a complication of polyarteritis nodosa. Rev Urol 9:235–238.
17. Teichman JM, Mattrey RF, Demby AM, Schmidt JD. 1993. Polyarteritis nodosa presenting as acute orchitis: a case report and review of the literature. J Urol 149:1139–1140. https://doi.org/10.1016/S0022-5347(17)36322-X.
18. Flaherty J, Bradley EL, III. 1999. Acute pancreatitis as a complication of polyarteritis nodosa. Int J Pancreatol 25:53–57. https://doi.org/10.1385/IJGC:25:1:53.
19. Yokoi Y, Nakamura I, Kaneko T, Sawayanagi T, Watahiki Y, Kuroda M. 2015. Pancreatic mass as an initial manifestation of polyarteritis nodosa: a case report and review of the literature. World J Gastroenterol 21:1014–1019. https://doi.org/10.3748/wjg.v21.i3.1014.
20. Churg J, Churg A. 1989. Idiopathic and secondary vasculitis: a review. Mod Pathol 2:144–160.
21. Lin J, Chen B, Wang JH, Zeng MS, Wang YX. 2006. Whole-body three-dimensional contrast-enhanced magnetic resonance (MR) angiography with parallel imaging techniques on a multichannel MR system for the detection of various systemic arterial diseases. Heart Vessels 21:395–398. https://doi.org/10.1007/s00380-006-0918-0.
22. Webb AA, Cullen CL, Lamont LA. 2006. Brainstem auditory evoked responses and ophthalmic findings in llamas and alpacas in Eastern Canada. Can Vet J 47:74–77.
23. Nakashima T, Naganawa S, Sone M, Tominaga M, Hayashi H, Yamamoto H, Liu X, Nuttall AL. 2003. Disorders of cochlear blood flow. Brain Res Brain Res Rev 43:17–28. https://doi.org/10.1016/S0165-0173(03)00189-9.
24. Jenkins HA, Pollak AM, Fisch U. 1981. Polyarteritis nodosa as a cause of sudden deafness. A human temporal bone study. Am J Otolaryngol 2:99–107. https://doi.org/10.1016/S0196-0709(81)80026-9.
25. Gussen P. 1977. Polyarteritis nodosa and deafness. A human temporal bone study. Arch Otorhinolaryngol 217:263–271. https://doi.org/10.1007/BF00465544.
26. Joglekar S, Deroee AF, Morita N, Cureoglu S, Schachern PA, Paparella M. 2010. Polyarteritis nodosa: a human temporal bone study. Am J Otolaryngol 31:221–225. https://doi.org/10.1016/j.amjoto.2009.02.006.
27. Wolf M, Kronenberg J, Engelberg S, Leventon G. 1987. Rapidly progressive hearing loss as a symptom of polyarteritis nodosa. Am J Otolaryngol 8:105–108. https://doi.org/10.1016/S0196-0709(87)80032-7.
28. Amor Dorado JC, Barreira Fernández MDP, Regueiro Villarin S, González-Gay MA. 2009. Audiovestibular manifestations in systemic vasculitis. Acta Otorrinolaringol Esp 60:432–442. (In Spanish.) https://doi.org/10.1016/j.otorri.2009.01.012.
29. Berrettini S, Ferri C, Ravecca F, LaCivita L, Bruschini L, Riente L, Mosca M, Sellari-Franceschini S. 1998. Progressive sensorineural hearing impairment in systemic vasculitides. Semin Arthritis Rheum 27:301–318. https://doi.org/10.1016/S0049-0172(98)80051-6.
30. Lightfoot RW, Jr, Michel BA, Bloch DA, Hunder GG, Zvaifler NJ, McShane DJ, Arend WP, Calabrese LH, Leavitt RY, Lie JT, Masi AT, Mills JA, Stevens MB, Wallace SL. 2010. The American College of Rheumatology 1990 criteria for the classification of polyarteritis nodosa. Arthritis Rheum 33:1088–1093. https://doi.org/10.1002/art.1780330805.
31. Jennette JC, Falk RJ, Bacon PA, Basu N, Cid MC, Ferrario F, Flores-Suarez LF, Gross WL, Guillevin L, Hagen EC, Hoffman GS, Jayne DR, Kallenberg CG, Lamprecht P, Langford CA, Luqmani RA, Mahr AD, Matteson EL, Merkel PA, Ozen S, Pusey CD, Rasmussen N, Rees AJ, Scott DG, Specks U, Stone JH, Takahashi K, Watts RA. 2013. 2012 revised International Chapel Hill Consensus Conference Nomenclature of Vasculitides. Arthritis Rheum 65:1–11. https://doi.org/10.1002/art.37715.
32. Jennette JC. 2013. Overview of the 2012 revised International Chapel Hill Consensus Conference Nomenclature of Vasculitides. Clin Exp Nephrol 17:603–606. https://doi.org/10.1007/s10157-013-0869-6.
33. Grau GE, Roux-Lombard P, Gysler C, Lambert C, Lambert PH, Dayer JM, Guillevin L. 1989. Serum cytokine changes in systemic vasculitis. Immunology 68:196–198.
34. Guillevin L. 2004. Virus-induced systemic vasculitides: new therapeutic approaches. Clin Dev Immunol 11:227–231. https://doi.org/10.1080/17402520400001744.
35. Saadoun D, Bieche I, Authier FJ, Laurendeau I, Jambou F, Piette JC, Vidaud M, Maisonobe T, Cacoub P. 2007. Role of matrix metalloproteinases, proinflammatory cytokines, and oxidative stress-derived molecules in hepatitis C virus-associated mixed cryoglobulinemia vasculitis neuropathy. Arthritis Rheum 56:1315–1324. https://doi.org/10.1002/art.22456.
36. Saadoun D, Bieche I, Maisonobe T, Asselah T, Laurendeau I, Piette JC, Vidaud M, Cacoub P. 2005. Involvement of chemokines and type 1 cytokines in the pathogenesis of hepatitis C virus-associated mixed cryoglobulinemia vasculitis neuropathy. Arthritis Rheum 52:2917–2925. https://doi.org/10.1002/art.21270.

37. Kikuchi K, Hoashi T, Kanazawa S, Tamaki K. 2005. Angiogenic cytokines in serum and cutaneous lesions of patients with polyarteritis nodosa. J Am Acad Dermatol 53:57–61. https://doi.org/10.1016/j.jaad.2005.02.018.
38. de Menthon M, Lambert M, Guiard E, Tognarelli S, Bienvenu B, Karras A, Guillevin L, Caillat-Zucman S. 2011. Excessive interleukin-15 transpresentation endows NKG2D+CD4+ T cells with innate-like capacity to lyse vascular endothelium in granulomatosis with polyangiitis (Wegener's). Arthritis Rheum 63:2116–2126. https://doi.org/10.1002/art.30355.
39. Abadie V, Jabri B. 2014. IL-15: a central regulator of celiac disease immunopathology. Immunol Rev 260:221–234. https://doi.org/10.1111/imr.12191.
40. Bobbala D, Chen XL, Leblanc C, Mayhue M, Stankova J, Tanaka T, Chen YG, Ilangumaran S, Ramanathan S. 2012. Interleukin-15 plays an essential role in the pathogenesis of autoimmune diabetes in the NOD mouse. Diabetologia 55:3010–3020. https://doi.org/10.1007/s00125-012-2675-1.
41. Miyagawa F, Tagaya Y, Kim BS, Patel HJ, Ishida K, Ohteki T, Waldmann TA, Katz SI. 2008. IL-15 serves as a costimulator in determining the activity of autoreactive CD8 T cells in an experimental mouse model of graft-versus-host-like disease. J Immunol 181:1109–1119. https://doi.org/10.4049/jimmunol.181.2.1109.
42. Di Sabatino A, Calarota SA, Vidali F, Macdonald TT, Corazza GR. 2011. Role of IL-15 in immune-mediated and infectious diseases. Cytokine Growth Factor Rev 22:19–33. https://doi.org/10.1016/j.cytogfr.2010.09.003.
43. Baslund B, Tvede N, Danneskiold-Samsoe B, Larsson P, Panayi G, Petersen J, Petersen LJ, Beurskens FJ, Schuurman J, van de Winkel JG, Parren PW, Gracie JA, Jongbloed S, Liew FY, McInnes IB. 2005. Targeting interleukin-15 in patients with rheumatoid arthritis: a proof-of-concept study. Arthritis Rheum 52:2686–2692. https://doi.org/10.1002/art.21249.
44. Kim YS, Maslinski W, Zheng XX, Stevens AC, Li XC, Tesch GH, Kelley VR, Strom TB. 1998. Targeting the IL-15 receptor with an antagonist IL-15 mutant/Fc gamma2a protein blocks delayed-type hypersensitivity. J Immunol 160:5742–5748.
45. Howland KC, Ausubel LJ, London CA, Abbas AK. 2000. The roles of CD28 and CD40 ligand in T cell activation and tolerance. J Immunol 164:4465–4470. https://doi.org/10.4049/jimmunol.164.9.4465.
46. Perez-Melgosa M, Hollenbaugh D, Wilson CB. 1999. CD40 ligand is a limiting factor in the humoral response to T cell-dependent antigens. J Immunol 163:1123–1127.
47. Kyburz D, Corr M, Brinson DC, Von Damm A, Tighe H, Carson DA. 1999. Human rheumatoid factor production is dependent on CD40 signaling and autoantigen. J Immunol 163:3116–3122.
48. Cervera R, Khamashta MA, Hughes GR. 1990. 'Overlap' syndromes. Ann Rheum Dis 49:947–948. https://doi.org/10.1136/ard.49.11.947.
49. Edington GM, White HA. 1972. The pathology of Lassa fever. Trans R Soc Trop Med Hyg 66:381–389. https://doi.org/10.1016/0035-9203(72)90268-4.
50. Knobloch J, McCormick JB, Webb PA, Dietrich M, Schumacher HH, Dennis E. 1980. Clinical observations in 42 patients with Lassa fever. Tropenmed Parasitol 31:389–398.
51. Walker DH, McCormick JB, Johnson KM, Webb PA, Komba-Kono G, Elliott LH, Gardner JJ. 1982. Pathologic and virologic study of fatal Lassa fever in man. Am J Pathol 107:349–356.
52. Winn WC, Jr, Monath TP, Murphy FA, Whitfield SG. 1975. Lassa virus hepatitis. Observations on a fatal case from the 1972 Sierra Leone epidemic. Arch Pathol 99:599–604.
53. Winn WC, Jr, Walker DH. 1975. The pathology of human Lassa fever. Bull World Health Organ 52:535–545.
54. Cashman KA, Broderick KE, Wilkinson ER, Shaia CI, Bell TM, Shurtleff AC, Spik KW, Badger CV, Guttieri MC, Sardesai NY, Schmaljohn CS. 2013. Enhanced efficacy of a codon-optimized DNA vaccine encoding the glycoprotein precursor gene of Lassa virus in a guinea pig disease model when delivered by dermal electroporation. Vaccines 1:262–277. https://doi.org/10.3390/vaccines1030262.
55. Cashman KA, Smith MA, Twenhafel NA, Larson RA, Jones KF, Allen RD, III, Dai D, Chinsangaram J, Bolken TC, Hruby DE, Amberg SM, Hensley LE, Guttieri MC. 2011. Evaluation of Lassa antiviral compound ST-193 in a guinea pig model. Antiviral Res 90:70–79. https://doi.org/10.1016/j.antiviral.2011.02.012.